Int J Thermophys (2010) 31:1259–1272
DOI 10.1007/s10765-010-0731-y

Acoustic Eigenvalues of Quasispherical Resonators: Beyond the Triaxial Ellipsoid Approximation

James B. Mehl

Received: 6 February 2010 / Accepted: 19 March 2010 / Published online: 13 April 2010

Abstract Quasispherical resonators are cavity resonators whose acoustic and electromagnetic modes are used in precision measurements, with shapes designed to split the $\ell = 1$ triplet modes to facilitate precise determination of the eigenfrequencies. The shapes can be represented in spherical coordinates by $r = a[1 - \varepsilon \mathscr{F}(\theta, \phi)]$ where $a \geq \max(r)$, $\varepsilon \ll 1$ is a positive scale parameter, and $\mathscr{F}$ is a non-negative function. Shape perturbation theory predicts that the fractional differences between the eigenvalues of the radial acoustic modes and the mean eigenvalues of the $\ell = 1$ triplet electromagnetic and acoustic modes can be written in the form $\mathscr{C}\varepsilon^2 + \mathscr{C}'\varepsilon^3 + \ldots$, where the coefficients $\mathscr{C}$ and $\mathscr{C}'$ depend on the multiplet. The coefficients $\mathscr{C}$ can be calculated analytically for acoustic modes for arbitrary QSR shapes. The third-order coefficient $\mathscr{C}'$ cannot be calculated analytically but has been determined using finite-element methods for some cases. This article shows how the acoustic values of $\mathscr{C}$ can be determined using the results of coordinate measuring machines.

Keywords Quasispherical resonator · Boundary shape perturbation · Acoustic thermometry · Boltzmann constant determination

1 Introduction

Quasispherical resonators (QSRs) are useful experimental tools for precision measurements of the speed of sound in gases [1], with applications in acoustic thermometry [1,2] and determination of the Boltzmann constant [3,4]. The measurement technique requires precise measurement of the eigenfrequencies of the radial ($\ell = 0$) acoustic

J. B. Mehl (✉)
P.O. Box 307, Orcas, WA 98280, USA
e-mail: jmehl@rockisland.com

modes and the triplet ($\ell = 1$) TM and TE electromagnetic modes. For a perfect spherical resonator of radius a, the eigenfrequencies equal

$$f_{\ell n}^{(\mathrm{A})} = \frac{c_{\mathrm{g}} \xi_{\ell n}^{(\mathrm{A})}}{2\pi a}, \quad f_{\ell n}^{(\mathrm{TM})} = \frac{c \xi_{\ell n}^{(\mathrm{TM})}}{2\pi a}, \quad f_{\ell n}^{(\mathrm{TE})} = \frac{c \xi_{\ell n}^{(\mathrm{TE})}}{2\pi a}. \tag{1}$$

Here c_{g} is the speed of sound in the gas, c is the speed of light, the eigenvalues $\xi_{\ell n}^{(\mathrm{A})}$ are solutions of $\mathrm{d}\, j_\ell(\xi)/\mathrm{d}\xi = 0$, the eigenvalues $\xi_{\ell n}^{(\mathrm{TM})}$ are solutions of $\mathrm{d}[\xi j_\ell(\xi)]/\mathrm{d}\xi = 0$, and the eigenvalues $\xi_{\ell n}^{(\mathrm{TE})}$ are solutions of $j_\ell(\xi) = 0$, where $j_\ell(\xi)$ is a spherical Bessel function, ℓ is the index of the spherical harmonic $Y_{\ell m}$ associated with the mode, and $n = 1, 2, \ldots$ enumerates the solutions. Radial ($\ell = 0$) solutions exist only for the acoustic case; the simplest electromagnetic modes are the threefold degenerate $\ell = 1$ triplets. If measurements with a perfect sphere were possible, the speed of sound could be determined by measuring the ratio of two eigenfrequencies, either as

$$\frac{c_{\mathrm{g}}}{c} = \frac{\xi_{\ell n}^{(\mathrm{TM})} f_{\ell n}^{(\mathrm{A})}}{\xi_{\ell n}^{(\mathrm{A})} f_{\ell n}^{(\mathrm{TM})}} \tag{2}$$

or a similar ratio with the TE eigenfrequency and eigenvalue.

Quasispherical resonators are commonly designed to have triaxial ellipsoidal shapes with relative axis lengths chosen so that the components of the $\ell = 1$ triplets are uniformly separated. This choice facilitates measurements [1]. The shapes of practical resonators may differ somewhat from the intended design, so it is of interest to know how small manufacturing errors affect the eigenvalues. For this purpose, it is useful to represent the shape in spherical coordinates by

$$r = a\,[1 - \varepsilon \mathscr{F}(\theta, \phi)] \tag{3}$$

where $a \geq \max(r)$, $\varepsilon \ll 1$ is a positive scale parameter, and $\mathscr{F}$ is a non-negative function. The perturbed eigenvalues ka of a QSR can be compared with the corresponding eigenvalues $\xi_{\ell n}^{\sigma}$ of of a reference sphere whose volume $4\pi(a')^3/3$ equals that of the QSR. (Here $\sigma = $ A, TM, or TE, indicates the mode type.) With the exception of the radial acoustic modes, the fractional eigenvalue difference is generally linear in ε. However, the mean eigenvalue of any multiplet satisfies [5,6]

$$\left\langle \frac{(ka)^2 - (\xi_{\ell n}^{\sigma})^2}{(\xi_{\ell n}^{\sigma})^2} \right\rangle = \mathscr{C}\varepsilon^2 + \mathscr{C}'\varepsilon^3 + \ldots. \tag{4}$$

This equation is also valid for the radial acoustic modes [7,8]. The coefficient $\mathscr{C}$ can be calculated for acoustic modes for any QSR shape [8,9]. For the electromagnetic modes it is known only for triaxial QSRs [10]. The coefficient $\mathscr{C}'$ cannot be calculated from shape perturbation theory as formulated by Morse and Feshbach [11]; selected values have been determined using finite-element models [9,10].

It would be most useful to determine how the values of $\mathscr{C}$ for electromagnetic modes depend on small departures from the known values for triaxial ellipsoids. In this article, the more limited result of determining $\mathscr{C}$ for the acoustic modes is obtained. Extension of the result to the electromagnetic modes will require a full, validated theory of the dependence of electromagnetic eigenvalues on arbitrary shapes similar to that of [9] for acoustic modes; that work has not been completed.

Coordinate measurement machines are being used to investigate the shapes of the parts used to fabricate QSRs [12]. The results can be expressed as a series of real spherical harmonics:

$$r = \sum_{\ell=0}^{\ell_{\max}} \sum_{m=-\ell}^{\ell} C_{\ell m} Y_{\ell m}(\theta, \phi). \tag{5}$$

The series can be compared with the expected series for a triaxial ellipsoid. It is of interest to see if deviations from a triaxial shape require significant corrections to the perturbation formulas for a true ellipsoid. This is worked out for the acoustic modes in the remainder of this article.

2 Shape Perturbation Theory

Equation 5 can be expressed in the form of Eq. 3 if the scale parameter ε is set to some arbitrary value on the order of $[\max(r) - \min(r)]/\max(r)$ and the shape function is written

$$\mathscr{F} = \sum_{\ell m} \alpha_{\ell m} Y_{\ell m}. \tag{6}$$

The two sets of expansion coefficients are related by

$$C_{00} = a(1 - \varepsilon\alpha_{00}); \quad C_{\ell m} = -\varepsilon a \alpha_{\ell m} \text{ for } \ell > 0. \tag{7}$$

With this choice it is straightforward to apply the formalism of [9] and calculate the coefficient $\mathscr{C}$ in Eq. 4.

Let the surface expressed by Eq. 3, designated S, lie within a perfect spherical surface S_0 of radius a, and let the regions within these surfaces be designated R and R_0, with the region between S and S_0 designated R'. The surfaces S and S_0 are assumed to be infinitely rigid and thermally insulating in the following. The acoustic modes in R_0 have eigenfunctions equal to the product of a spherical Bessel function and a spherical harmonic;

$$\Phi_{\ell nm} = j_\ell(k_{\ell n} r) Y_{\ell m}(\theta, \phi). \tag{8}$$

The corresponding eigenvalues $k_{\ell n}^2$ equal $(\xi_{\ell n}/a)^2$, where $\xi_{\ell n}$ is the nth root of $j'_\ell(\xi) = 0$. These modes are $(2\ell + 1)$-fold degenerate. In order to use them as the unperturbed modes of the QSR, it is necessary to form appropriate linear combinations of the members of each degenerate multiplet, chosen so that the quantities [9, Eq. 15],

$$A_{\ell nm,\ell nm'} = \int\limits_{R'} \left[k_{\ell n}^2 \Phi_{\ell nm} \Phi_{\ell nm'} - \nabla \Phi_{\ell nm} \cdot \nabla \Phi_{\ell nm'}\right] \mathrm{d}V \tag{9}$$

form a diagonal matrix of dimension $(2\ell + 1)$. Within R', the spherical Bessel functions have a radial derivative $j'_\ell(k_{\ell n} r)$ of order ε, so the functions can be approximated by [9, Eq. 17]

$$j_\ell(k_{\ell n} r) = j_\ell(\xi_{\ell n}) + O(\varepsilon^2), \tag{10}$$

and Eq. 9 by

$$\frac{A_{\ell nm,\ell nm'}}{[j_\ell(\xi_{\ell n})]^2} = \varepsilon a^3 \int \left[\xi_{\ell n}^2 Y_{\ell m} Y_{\ell m'} (1 - \varepsilon \mathscr{F}) - (r \nabla Y_{\ell m}) \cdot (r \nabla Y_{\ell m'})\right] \mathscr{F} \,\mathrm{d}\Omega + O(\varepsilon^3), \tag{11}$$

where $\mathrm{d}\Omega$ is an element of solid angle. (In this equation, the operator $r\nabla$ operates only on the angular variables.) Equation 11 is developed further in the next sections. The remainder of this section summarizes the formulas necessary to compute the acoustic eigenfrequencies through order ε^2 under the assumption that the unperturbed modes are chosen so that Eq. 11 is diagonal.

In Ref. [9] the shape function was divided into two terms $\mathscr{F} = \mathscr{F}_0 + \varepsilon \mathscr{F}_1$; this separation is not useful when dealing with shapes defined by CMM data. Accordingly, the substitutions $\mathscr{F}_0 = \mathscr{F}$ and $\mathscr{F}_1 = 0$ should be made in equations from [9].

Consider the modes of the spherical cavity R. As ε increases from 0, the eigenvalues and eigenfunctions of each mode start with the values for cavity R_0 and evolve in a way that can be expressed as a power series in ε. Instead of comparing the eigenvalues k^2 for finite ε with the corresponding eigenvalues of R_0, it is more useful to compare them with the corresponding eigenvalues of a reference sphere whose volume equals the volume of the QSR. The fractional difference is [9, Eq. 32]

$$\begin{aligned}\frac{(ka')^2 - \xi_{\ell n}^2}{\xi_{\ell n}^2} &= \frac{A_{\ell nm\ell nm}}{k_{\ell n}^2 N_{\ell nm}} + \frac{4\varepsilon^2}{\xi_{\ell n}^2 - \ell(\ell+1)} \sum_{\ell' m'} |B_{\ell m \ell' m'}^{(n)}|^2 \mathscr{S}_{\ell n \ell'} \\ &\quad + \frac{2\varepsilon^2 |B_{\ell m00}^{(n)}|^2}{\xi_{\ell n}^2 [\xi_{\ell n}^2 - \ell(\ell+1)]} - 2\varepsilon \langle \mathscr{F} \rangle + \varepsilon^2 \left[-\langle \mathscr{F} \rangle^2 + 2\langle \mathscr{F}^2 \rangle\rangle\right] \\ &\quad - 2\varepsilon \langle \mathscr{F} \rangle \frac{A_{\ell nm\ell nm}}{k_{\ell n}^2 N_{\ell nm}} + O(\varepsilon^3),\end{aligned} \tag{12}$$

where a' is the radius of the reference sphere and the triangular brackets $\langle\cdot\rangle$ indicate an average over solid angle. The first term in Eq. 12 is, with

$$N_{\ell nm} = \frac{a^3}{2}[j_\ell(\xi_{\ell n})]^2\left[1 - \frac{\ell(\ell+1)}{\xi_{\ell n}^2}\right] - \varepsilon a^3[j_\ell(\xi_{\ell n})]^2\int \mathscr{F}|Y_{\ell m}|^2\,\mathrm{d}\Omega + O(\varepsilon^2) \tag{13}$$

for the denominator and Eq. 11 for the numerator, equal to

$$\frac{A_{\ell nm\ell nm}}{k_{\ell n}^2 N_{\ell nm}} = 2\varepsilon\frac{\int\left[\xi_{\ell n}^2 Y_{\ell m}^2(\mathscr{F} - \varepsilon\mathscr{F}^2) - |r\nabla Y_{\ell m}|^2\mathscr{F}\right]\mathrm{d}\Omega}{\xi_{\ell n}^2 - \ell(\ell+1) - 2\varepsilon\xi_{\ell n}^2\int\mathscr{F}|Y_{\ell m}|^2\,\mathrm{d}\Omega} + O(\varepsilon^3). \tag{14}$$

The other quantities in Eq. 12 are

$$B_{\ell m\ell' m'}^{(n)} = \int\left[\xi_{\ell n}^2 Y_{\ell' m'}Y_{\ell m} - r^2\nabla Y_{\ell' m'}\cdot\nabla Y_{\ell m}\right]\mathscr{F}\,\mathrm{d}\Omega \tag{15}$$

and the quantities $\mathscr{S}_{\ell n\ell'}$, infinite sums which are evaluated analytically in [9] to obtain, [9, Eqs. 26, 27], for $\ell' \neq 0$,

$$\mathscr{S}_{\ell n\ell'} = \begin{cases} -\dfrac{j_{\ell'}(\xi_{\ell n})}{2\xi_{\ell n}j'_{\ell'}(\xi_{\ell n})}, & \text{for } \ell' \neq \ell \\ \dfrac{\xi_{\ell n}^2 - 3\ell(\ell+1)}{4[\xi_{\ell n}^2 - \ell(\ell+1)]^2}, & \text{for } \ell' = \ell, \end{cases} \tag{16}$$

and for $\ell' = 0$,[1]

$$\mathscr{S}_{\ell n0} = \begin{cases} -\dfrac{1}{2\xi_{\ell n}^2} - \dfrac{j_0(\xi_{\ell n})}{2\xi_{\ell n}j'_0(\xi_{\ell n})}, & \text{for } \ell \neq 0, \\ -1/(4\xi_{0n}^2), & \text{for } \ell = 0. \end{cases} \tag{17}$$

When $\mathscr{F}$ is expressed as the series (Eq. 6), the required average values are

$$\langle\mathscr{F}\rangle = \frac{\alpha_{00}}{\sqrt{4\pi}}, \qquad \left\langle\mathscr{F}^2\right\rangle = \frac{1}{4\pi}\sum_{\ell' m'}\alpha_{\ell' m'}^2. \tag{18}$$

2.1 Radial Modes

For $\ell = 0$, Eq. 12 can be simplified using

$$B_{00\ell' m'}^{(n)} = \xi_{0n}^2\int Y_{\ell' m'}Y_{00}\mathscr{F}\,\mathrm{d}\Omega = \xi_{0n}^2\alpha_{\ell' m'}/\sqrt{4\pi}, \tag{19}$$

$$\frac{A_{0n00n0}}{k_{0n}^2 N_{0n0}} = 2\varepsilon\left[\langle\mathscr{F}\rangle - \varepsilon\langle\mathscr{F}^2\rangle + 2\varepsilon\langle\mathscr{F}\rangle^2\right] + O(\varepsilon^3), \tag{20}$$

[1] A typo in Ref. [9], where the sign of the second term in the first line of Eq. 17 was incorrectly printed "+", is corrected here.

and the second of Eq. 17 to obtain

$$\frac{(ka')^2 - \xi_{0n}^2}{\xi_{0n}^2} = \frac{\varepsilon^2 \xi_{0n}^2}{\pi} \sum_{\ell=1}^{\infty} \sum_{m=-\ell}^{\ell} \alpha_{\ell m}^2 \mathscr{S}_{0n\ell}. \tag{21}$$

2.2 Nonradial $\ell = 1$ Modes

The first step of the perturbation calculation for nonradial modes is proper choice of the unperturbed states. Consider the square matrix $\boldsymbol{\Lambda}^{(\mathrm{a}\ell n)}$ of dimension $2\ell + 1$ associated with the ℓn multiplet, with elements defined as

$$\Lambda_{mm'}^{(\mathrm{a}\ell n)} = 2\varepsilon \frac{\int [\xi_{\ell n}^2 Y_{\ell m} Y_{\ell m'} - r^2 \nabla Y_{\ell m} \cdot \nabla Y_{\ell m'}] \mathscr{F} \, \mathrm{d}\Omega}{\xi_{1n}^2 - 2} - 2\varepsilon \delta_{mm'} \langle \mathscr{F} \rangle, \tag{22}$$

defined so that the diagonal terms equal the terms of order ε in the perturbation series (Eq. 12); the eigenvalues of this matrix equal the left-hand side of Eq. 12 to order ε. Diagonalizing this submatrix insures that Eq. 11 is diagonal to $O(\varepsilon)$; it will be diagonal to $O(\varepsilon^2)$ if the matrix formed by adding elements,

$$\varepsilon \nu_{mm'} = \frac{-2\varepsilon^2 \xi_{1n}^2}{\xi_{1n}^2 - 2} \int Y_{1m} Y_{1m'} \mathscr{F}^2 \, \mathrm{d}\Omega \tag{23}$$

to $\boldsymbol{\Lambda}^{(\mathrm{a}1n)}$ is also diagonal.

For simplicity, the superscript $a1n$ on the matrix $\boldsymbol{\Lambda}^{a1n}$ is dropped in the following. Suppose $\boldsymbol{\Lambda}$ has been diagonalized so that its eigenvalues are simply the diagonal element with eigenvalues Λ_{mm}; consider the sum of $\boldsymbol{\Lambda}$ and a general matrix $\varepsilon \Delta \boldsymbol{\Lambda}$ with elements $\varepsilon \nu_{mm'}$. Note that $\Lambda_{mm} \propto \varepsilon$ because of the prefactor in Eq. 22, so the eigenvalues Λ' of the full matrix will equal the Λ_{mm} plus a correction of order ε^2; this consideration motivates the notation for the elements of $\varepsilon \Delta \boldsymbol{\Lambda}$. The eigenvalues of the full matrix are the roots of the characteristic polynomial formed by setting the determinant of $\boldsymbol{\Lambda} + \varepsilon \Delta \boldsymbol{\Lambda}$ equal to zero:

$$\begin{vmatrix} \Lambda_{11} + \varepsilon \nu_{11} - \Lambda' & \varepsilon \nu_{10} & \varepsilon \nu_{1,-1} \\ \varepsilon \nu_{01} & \Lambda_{00} + \varepsilon \nu_{00} - \Lambda' & \varepsilon \nu_{0,-1} \\ \varepsilon \nu_{-1,1} & \varepsilon \nu_{-1,0} & \Lambda_{-1,-1} + \varepsilon \nu_{-1,-1} - \Lambda' \end{vmatrix} = 0. \tag{24}$$

When this is expanded and terms of order ε^3 and higher are dropped, the characteristic polynomial takes the trivial form,

$$\left(\Lambda_{11} + \varepsilon \nu_{11} - \Lambda'\right) \left(\Lambda_{00} + \varepsilon \nu_{00} - \Lambda'\right) \left(\Lambda_{-1,-1} + \varepsilon \nu_{-1,-1} - \Lambda'\right) = 0. \tag{25}$$

The eigenvalues are simply shifted from Λ_{mm} to $\Lambda_{mm} + \varepsilon \nu_{mm}$. *More importantly, the eigenvectors are not affected in this order.* Once the unperturbed eigenvectors are chosen so that $\mathbf{\Lambda}$ is diagonal, the eigenvalue perturbations can be calculated to second order by simply evaluating the contributions to Eq. 12.

When the series in Eq. 6 is inserted in Eq. 22, the matrix elements are

$$\Lambda_{mm'}^{(\mathrm{a}\ell n)} = 2\varepsilon \sum_{\ell'' m''} \alpha_{\ell'' m''} \frac{\int \left[\xi_{\ell n}^2 Y_{\ell m} Y_{\ell m'} - r^2 \nabla Y_{\ell m} \cdot \nabla Y_{\ell m'}\right] Y_{\ell'' m''} \, \mathrm{d}\Omega}{\xi_{1n}^2 - 2} - 2\varepsilon \delta_{mm'} \frac{\alpha_{00}}{\sqrt{4\pi}}. \tag{26}$$

The integrals are of the Gaunt type, which can be expressed as linear combinations of integrals over products of three complex spherical harmonics. For $\ell = 1$, the only nonvanishing terms in the series (Eq. 26) are those with $\ell'' = 0$ and $\ell'' = 2$. The matrix for this case takes the particularly simple form,

$$\mathbf{\Lambda}^{(\mathrm{a}1n)} = \frac{\varepsilon}{2\sqrt{5\pi}} \frac{\xi_{1n}^2 + 1}{\xi_{1n}^2 - 2} \begin{bmatrix} -\alpha_{20} + \sqrt{3}\alpha_{22} & \sqrt{3}\alpha_{21} & \sqrt{3}\alpha_{2,-2} \\ \sqrt{3}\alpha_{21} & 2\alpha_{20} & -\sqrt{3}\alpha_{2,-1} \\ \sqrt{3}\alpha_{2,-2} & -\sqrt{3}\alpha_{2,-1} & -\alpha_{20} - \sqrt{3}\alpha_{22} \end{bmatrix}. \tag{27}$$

Note that matrices identical to this except for the numerical prefactors apply to the TM and TE electromagnetic modes [1], for which the present discussion is thus applicable.

Diagonalization of Eq. 27 is straightforward. The original set of real spherical harmonics equals

$$\begin{aligned} Y_{11} &= \frac{1}{2}\sqrt{\frac{3}{\pi}} \sin\theta \sin\phi = \frac{1}{2}\sqrt{\frac{3}{\pi}} \frac{x}{r}, \\ Y_{10} &= \frac{1}{2}\sqrt{\frac{3}{\pi}} \cos\theta = \frac{1}{2}\sqrt{\frac{3}{\pi}} \frac{z}{r}, \\ Y_{1,-1} &= \frac{1}{2}\sqrt{\frac{3}{\pi}} \sin\theta \cos\phi = \frac{1}{2}\sqrt{\frac{3}{\pi}} \frac{y}{r}. \end{aligned} \tag{28}$$

The orthogonal transformation that diagonalizes $\mathbf{\Lambda}^{(\mathrm{a}1n)}$ can be regarded as a rotation in the Cartesian space xyz. Let $\mathbf{Q}$ be a matrix whose columns equal the eigenvectors, so that $\mathbf{Q}^T \mathbf{\Lambda}^{(\mathrm{a}1n)} \mathbf{Q}$ is diagonal. This is equivalent to transforming the basis vectors with

$$\begin{bmatrix} Y_{11} \\ Y_{10} \\ Y_{1,-1} \end{bmatrix} = \mathbf{Q} \begin{bmatrix} Y'_{11} \\ Y'_{10} \\ Y'_{1,-1} \end{bmatrix}. \tag{29}$$

Alternatively, consider the rotation of the coordinates,

$$\begin{bmatrix} x \\ z \\ y \end{bmatrix} = \mathbf{Q} \begin{bmatrix} x' \\ z' \\ y' \end{bmatrix}. \tag{30}$$

This orthogonal transformation preserves the lengths of vectors, so $r = r'$, and thus Eq. 30 together with Eqs. 28 is equivalent to Eq. 29.

To summarize, step one of the perturbation calculation requires diagonalization of the matrix $\boldsymbol{\Lambda}^{(\mathrm{a}1n)}$, then using the eigenvectors to form the matrix $\mathbf{Q}$ and rotating the original coordinates with the inverse of Eq. 30 to get a modified representation of the shape in which $\boldsymbol{\Lambda}^{(\mathrm{a}1n)}$ is diagonal. This means that the only $\ell = 2$ terms in the expansion in the rotated coordinate system will be α_{20} and $\alpha_{2,\pm 2}$. This can always be done, and it will simplify the rest of the computations.

3 BCU3

The diagonalization procedure described in Sect. 2.2 was carried out using the coefficients from the harmonic decomposition of the QSR designated BCU3 [13]. The design geometry of BCU3 was an ellipsoid with semi-axes equal to (50.0, 49.975, 49.95) mm. The original expansion coefficients (Fig. 1, top) were used to diagonalize the matrix $\boldsymbol{\Lambda}^{(\mathrm{a}1n)}$ and find the eigenvectors. The latter were then used to rotate the CMM data, and a new harmonic decomposition was carried out. The rotation axis was $[-0.5618, 0.0995, -0.8213]^{\mathrm{T}}$, the angle was 1.84°. The coefficients $\alpha_{\ell m}$ of the second fit are plotted in Fig. 1, bottom.

For comparison, Fig. 1 also displays the coefficients for an erect ellipsoid with semi-axes scaled according to $a_y = a_x(1 + \varepsilon_2)$ and $a_z = a_x(1 + \varepsilon_1)$. This shape has a harmonic decomposition in the form defined by Eqs. 3 and 6 with

$$\begin{aligned}
\alpha_{00} &= \frac{4}{3}\sqrt{\pi}\,(\varepsilon_1 + \varepsilon_2) - \frac{2}{15}\sqrt{\pi}\left(7\varepsilon_1^2 + 8\varepsilon_1\varepsilon_2 + 7\varepsilon_2^2\right),\\
\alpha_{20} &= \frac{2}{3}\sqrt{\frac{\pi}{5}}\,(2\varepsilon_1 - \varepsilon_2) - \frac{a}{7}\sqrt{\frac{\pi}{7}}\left(2\varepsilon_1^2 - 2\varepsilon_1\varepsilon_2 - \varepsilon_2^2\right),\\
\alpha_{22} &= -2\sqrt{\frac{\pi}{15}}\varepsilon_2 - \frac{a}{7}\sqrt{\frac{3\pi}{5}}\,(2\varepsilon_1 - \varepsilon_2)\,\varepsilon_2,\\
\alpha_{40} &= \frac{\sqrt{\pi}}{35}\left(8\varepsilon_1^2 - 8\varepsilon_1\varepsilon_2 + 3\varepsilon_2^2\right),\\
\alpha_{42} &= -\frac{2\sqrt{5\pi}}{35}\,(2\varepsilon_1 - \varepsilon_2)\,\varepsilon_2,\\
\alpha_{44} &= \sqrt{\frac{\pi}{35}}\varepsilon_2^2.
\end{aligned} \tag{31}$$

The ellipsoidal values displayed in Fig. 1 correspond to [13]

$$\varepsilon_1 = 0.00108796, \qquad \varepsilon_2 = 0.00050524, \tag{32}$$

obtained from the splitting of the electromagnetic triplets. Comparison of the top and bottom panels of Fig. 1 shows that the rotation has zeroed out the values of α_{2m} that are not consistent with Eq. 31. However, there are many terms in the lower panel that

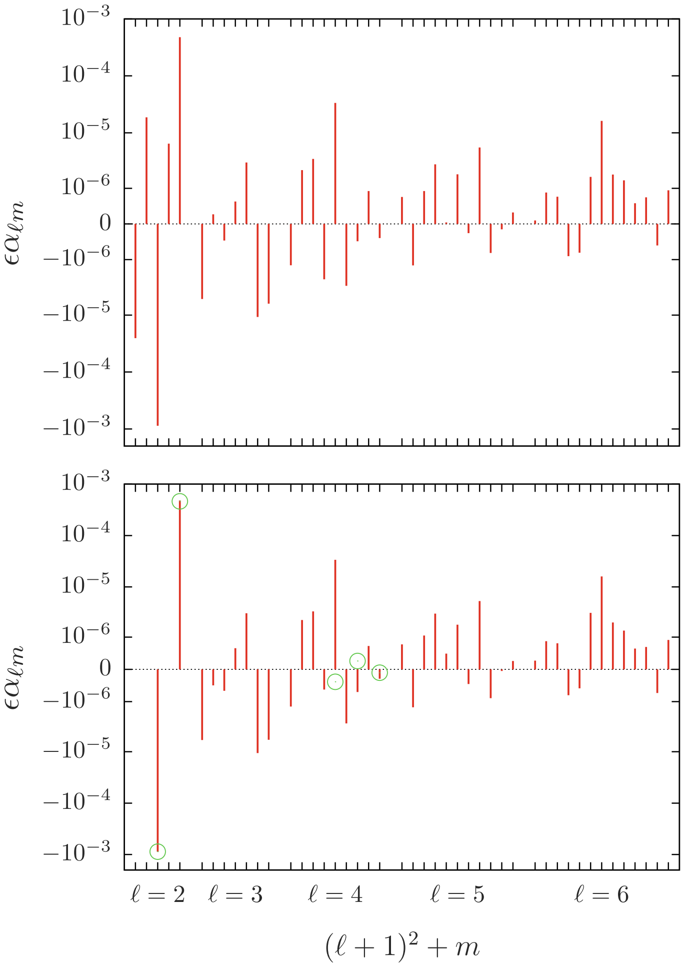

Fig. 1 *Top*: coefficients $\varepsilon\alpha_{\ell m}$ calculated from fits of Eq. 5 to CMM measurements on the QSR BCU3. Equation 7 is used to relate the fit coefficients $C_{\ell m}$ to the $\varepsilon\alpha_{\ell m}$ using the value $a = 50.00027$ mm. The abscissa is $\ell(\ell+1)+m$, which maps the pairs ℓ, m into a linear series with unit gaps between the multiplets; the axis labels ℓ are at $\ell(\ell + 1)$, i.e., the center of the ℓ-multiplet. The ordinate is scaled proportional to arcsinh$(2000 \cdot \varepsilon\alpha_{\ell m})$; this choice makes the scaling linear for small $|2000 \cdot \varepsilon\alpha_{\ell m}|$ and proportional to $\pm \log |2000 \cdot \varepsilon\alpha_{\ell m}|$ for large arguments. *Bottom*: the same quantities after rotation of the CMM data. The *open circles* are values calculated for an erect ellipsoid with values of ε_1 and ε_2 from the triplet splittings. Note that the only strong components of both the CMM fit and the ellipsoid are α_{20} and α_{22}; for which there is good agreement between the ellipsoid and CMM values. However, the magnitudes of the higher-ℓ CMM coefficients exceed the values calculated for an ellipsoid

are inconsistent with the triaxial ellipsoidal shape. The effects of these terms on the acoustic eigenvalues will be calculated in the following.

Once the CMM data are rotated and a diagonal submatrix is obtained as described above, the remaining calculations are straightforward. They can be carried out best with a symbolic program like Maple or Mathematica.

The diagonal form of the numerator of the first term in Eq. 12 can be evaluated using Eq. 11 to obtain

$$\frac{A_{\ell nm,\ell nm}}{[j_\ell(\xi_{\ell n})]^2} = \varepsilon a^3 \int \left[\xi_{\ell n}^2 Y_{\ell m}^2 - (r\nabla Y_{\ell m})\cdot(r\nabla Y_{\ell m'})\right] \mathscr{F}\, \mathrm{d}\Omega - \varepsilon^2 a^3 \int \xi_{\ell n}^2 Y_{\ell m}^2 \mathscr{F}^2\, \mathrm{d}\Omega + O(\varepsilon^3). \tag{33}$$

The first term has already been evaluated in the calculation of the matrix $\mathbf{\Lambda}_{mm}^{a1n}$; once that matrix has been diagonalized the only contributions come from α_{00}, α_{20}, and α_{22}. The second integral can be evaluated using the substitutions,

$$Y_{1,\pm1}^2 = \frac{Y_{00}}{\sqrt{4\pi}} - \frac{1}{10}\sqrt{\frac{5}{\pi}}Y_{20} \pm \frac{1}{10}\sqrt{\frac{15}{\pi}}Y_{22}, \quad Y_{10}^2 = \frac{Y_{00}}{\sqrt{4\pi}} + \frac{1}{5}\sqrt{\frac{5}{\pi}}Y_{20}, \tag{34}$$

to obtain

$$\int Y_{1,\pm1}^2 \mathscr{F}^2\, \mathrm{d}\Omega = \frac{\alpha_{00}^2}{4\pi} - \frac{1}{\sqrt{20\pi}} \sum_{\ell' m' \ell'' m''} \alpha_{\ell' m'}\alpha_{\ell'' m''} \int [Y_{20} \pm \sqrt{3} Y_{22}] Y_{\ell' m'} Y_{\ell'' m''}\, \mathrm{d}\Omega \tag{35}$$

and

$$\int Y_{10}^2 \mathscr{F}^2\, \mathrm{d}\Omega = \frac{\alpha_{00}^2}{4\pi} + \frac{1}{\sqrt{5\pi}} \sum_{\ell' m' \ell'' m''} \alpha_{\ell' m'}\alpha_{\ell'' m''} \int Y_{20} Y_{\ell' m'} Y_{\ell'' m''}\, \mathrm{d}\Omega. \tag{36}$$

The integrals over the product of three real spherical harmonics appearing here are of the Gaunt type. They vanish unless $\ell' + \ell'' + 2$ is an even integer satisfying $|\ell' - 2| \le \ell'' \le \ell' + 2$. The lower limits of the sums over ℓ'' in Eqs. 35 and 36 equal 2 for $\ell' = 0$, 1 for $\ell' = 1$, and $\ell' - 2$ for $\ell' \ge 2$. This means that the sums in Eqs. 35 and 36 are limited to

$$\sum_{\ell'=0}^{\ell_{\max}} \sum_{m'=-\ell'}^{\ell'} \sum_{\ell''=-|\ell'-2|}^{\ell'+2} \sum_{m''=-\ell''}^{\ell''} (\bullet). \tag{37}$$

Equations 34 can also be used in evaluating the $O(\varepsilon)$ term in Eq. 13; the normalization integrals then equal

$$\frac{k_{1n}^2 N_{1nm}}{[j_1(\xi_{1n})]^2} = \frac{a}{2}\left[\xi_{1n}^2 - 2\right] - 2\varepsilon a \xi_{1n}^2 \begin{cases} \dfrac{\alpha_{00}}{\sqrt{4\pi}} - \dfrac{\alpha_{20}}{\sqrt{20\pi}} \pm \dfrac{\sqrt{3}\alpha_{22}}{\sqrt{20\pi}}, & m = \pm 1 \\ \dfrac{\alpha_{00}}{\sqrt{4\pi}} + \dfrac{2\alpha_{20}}{\sqrt{20\pi}}, & m = 0 \end{cases} + O(\varepsilon^2). \tag{38}$$

Expansion of Eq. 15 yields

$$B^{(n)}_{1m\ell'm'} = \sum_{\ell''m''} \alpha_{\ell''m''} \int \xi^2_{1n} Y_{1m} Y_{\ell m'} - r^2 \nabla Y_{1m} \cdot \nabla Y_{\ell'm'}] Y_{\ell''m''}\, \mathrm{d}\Omega$$
$$= \sum_{\ell''m''} \alpha_{\ell''m''} \left[\xi^2_{\ell n} - \frac{\ell''(\ell''+1) - \ell'(\ell'+1) - 2}{2} \right] \int Y_{1m} Y_{\ell'm'} Y_{\ell''m''}\, \mathrm{d}\Omega \tag{39}$$

In the second line, the integral involving the gradients of the spherical harmonics was simplified; this simplification can be made using the technique described in the Appendix of [5], or, alternatively, using the raising and lowering angular momentum operators [14, Chap. 9]. The triple-spherical harmonic integral vanishes unless $\ell' + \ell'' + 1$ is an even integer satisfying $|\ell' - 1| \leq \ell'' \leq \ell' + 1$. Accordingly, there are only a limited number of terms (maximum 6) contributing to

$$B^{(n)}_{1m\ell'm'} = \sum_{m'=-|\ell'-1|}^{|\ell'-1|} \alpha_{\ell'-1,m''} \left[\xi^2_{\ell n} + \ell' + 1 \right] \int Y_{1m} Y_{\ell'm'} Y_{\ell'-1,m''}\, \mathrm{d}\Omega$$
$$+ \sum_{m''=-\ell'-1}^{\ell'+1} \alpha_{\ell'+1,m''} \left[\xi^2_{\ell n} - \ell' \right] \int Y_{1m} Y_{\ell'm'} Y_{\ell'+1,m''}\, \mathrm{d}\Omega. \tag{40}$$

It follows that the upper limit of the sum in the second term of Eq. 12 can be set to $\ell_{\max} + 1$.

4 Some Numerical Results

Use of CMM data for calculating the eigenvalue perturbations of radial modes requires only substitution in Eq. 21 and will not be considered further here.

Additional terms can be included in the perturbation series for $\ell = 1$ following these guidelines.

1. Use a symbolic algebra program.
2. Evaluate the first term in the perturbation series.
3. Identify the index $\ell_{\max}$ of the highest-order significant coefficient $\alpha_{\ell'm'}$.
4. Evaluate Eq. 40 for ℓ' up to $\ell_{\max} + 1$, and sum the contributions to the second term in Eq. 12 for $\ell \leq \ell_{\max} + 1$.
5. The full perturbation series can then be evaluated.

Consider some examples. Table 1 lists the CMM values of $\alpha_{\ell m}$ with the largest magnitudes.

Table 1 Largest magnitude coefficients $\alpha_{\ell m}$ in harmonic decomposition of the CMM measurements on BCU3

ℓ	m	$10^3 \cdot \alpha_{\ell m}$	$U\left(10^3 \cdot \alpha_{\ell m}\right)$	$10^3 \cdot \alpha_{\ell m,\text{Ellipsoid}}$
2	0	−0.87767	0.00017	−0.88134
2	2	0.47922	0.00021	0.46187
4	0	0.03364	0.00018	−0.00030
6	0	0.01597	0.00015	
3	2	−0.01062	0.00019	
3	−3	−0.00591	0.00022	
3	3	−0.00587	0.00022	
5	2	0.00530	0.00018	
4	−2	0.00333	0.00020	0.00019
6	−1	0.00311	0.00016	
3	1	0.00305	0.00019	
5	−2	0.00300	0.00018	
4	1	−0.00279	0.00018	
4	−3	0.00224	0.00020	
6	1	0.00201	0.00016	
5	0	0.00182	0.00015	
6	2	0.00137	0.00018	
5	−4	−0.00132	0.00020	
4	−4	−0.00128	0.00022	
5	−3	0.00108	0.00019	
6	6	0.00086	0.00022	
5	3	−0.00084	0.00019	
		...		
4	2	−0.00060	0.00019	0.00019
4	4	−0.00022	0.00022	−0.00008

The theoretical values for an ellipsoid with the parameters of Eq. 32 are shown for comparison. The uncertainties in the coefficients as determined in the fits are listed in the fourth column. Note that α_{42} and α_{44} have large fractional uncertainties; they are included in the table for comparison with the ellipsoid values

Figure 1 and Table 1 indicate that the largest correction to the triaxial ellipsoid shape is the term $\varepsilon_{40} Y_{40}$. When this term is added to $\mathscr{F}$, the calculated mode average is

$$\left\langle \frac{(ka')^2 - \xi_{1n}^2}{\xi_{1n}^2} \right\rangle_{1n} = \frac{8\left(3\xi_{1n}^8 - 14\xi_{1n}^6 + 90\xi_{1n}^4 - 243\xi_{1n}^2 + 10\right)}{1125\left(\xi_{1n}^2 - 2\right)^3}\left(\varepsilon_1^2 - \varepsilon_1\varepsilon_2 + \varepsilon_2^2\right) + \frac{9\xi_{1n}^{10} - 473\xi_{1n}^8 + 4879\xi_{1n}^6 - 21638\xi_{1n}^4 + 57820\xi_{1n}^2 - 88200}{70\pi\left(\xi_{1n}^2 - 2\right)\left(2\xi_{1n}^4 - 71\xi_{1n}^2 + 270\right)\left(\xi_{1n}^2 - 4\right)}\varepsilon_{40}^2 + O\left(\varepsilon^3\right), \quad (41)$$

the sum of the known quadratic term for ellipsoids [9] and a small correction (0.5 % for $n = 1$, much less for higher modes). The other large terms in Table 1 can be treated similarly. Because the algebraic representation of the results quickly becomes much more complex than Eq. 41, only numerical results are presented here. Table 2 lists the

Table 2 Contributions to the mode-average eigenvalue perturbations for the $1n$ acoustic triplets in ppm $\left(10^{-6}\right)$

n	Ellipsoid	Y_{40}	Y_{60}^{2}	Y_{32}	Sum of 3	Sum of 6
1	0.2816	−0.0009	−0.0002	−0.0001	−0.0013	−0.0014
2	0.7098	−0.0010	−0.0007	0.0004	−0.0013	−0.0009
3	1.6390	0.0016	0.0020	−0.0002	0.0035	0.0034
4	2.9476	0.0033	−0.0001	−0.0001	0.0031	0.0033
5	4.6317	0.0054	0.0002	−0.0001	0.0056	0.0053
6	6.6908	0.0080	0.0005	−0.0001	0.0084	0.0082
7	9.1245	0.0110	0.0008	−0.0001	0.0117	0.0116
8	11.9328	0.0145	0.0011	−0.0001	0.0155	0.0154
9	15.1156	0.0185	0.0015	−0.0001	0.0199	0.0197
10	18.6729	0.0229	0.0019	−0.0001	0.0247	0.0246

separate effects of including the terms with (ℓ, m) equal to $(4, 0)$, $(6, 0)$, and $(3, 0)$; the total effect of these three terms, and finally, the total effect of these three terms and terms with (ℓ, m) equal to $(3, 3)$, $(3, -3)$, and $(5, 2)$. The table also lists the value for the ellipsoidal shape. In all cases, the corrections to the ellipsoidal shape are very small.

5 Summary

A formalism that can be used for calculating the $\ell = 0$ and $\ell = 1$ acoustic eigenvalues to order ε^2 has been described in sufficient detail that similar calculations can be carried out for any QSR whose shape is known from CMM measurements.

Acknowledgments This work was begun while the author was a guest at the Laboratoire Commun de Métrologie LNE/Cnam, La Plaine Saint Denis, France, whose support is gratefully acknowledged. The author also thanks Laurent Pitre for his support and for some stimulating discussions.

References

1. J.B. Mehl, M.R. Moldover, L. Pitre, Metrologia **41**, 295 (2004)
2. L. Pitre, M.R. Moldover, W.L. Tew, Metrologia **43**, 142 (2006)
3. R.M. Gavioso, G. Benedetto, P.A.G. Albo, A. Merlone, A. Balsamo, G.E. D'Errico, R. Spagnolo, Int. J. Thermophys. **28**, 1775 (2007)
4. L. Pitre, C. Guianvarc'h, F. Sparasci, A. Richard, D. Truong, Int. J. Thermophys. **29**, 1730 (2008)
5. J.B. Mehl, J. Acoust. Soc. Am. **79**, 278 (1986)
6. J.B. Mehl, M.R. Moldover, Phys. Rev. A **34**, 3341 (1986)
7. M.R. Moldover, J.B. Mehl, M. Greenspan, J. Acoust. Soc. Am. **79**, 253 (1986)
8. J.B. Mehl, J. Acoust. Soc. Am. **71**, 1109 (1982)
9. J.B. Mehl, J. Res. Natl Inst. Stand. Technol. **112**, 163 (2007)
10. J.B. Mehl, Metrologia **46**, 554 (2009)
11. P.M. Morse, H. Feshbach, *Methods of Theoretical Physics, Part II* (McGraw-Hill, New York, 1953), p. 1052

12. M. de Podesta, E.F. May, J.B. Mehl, L. Pitre, R.M. Gavioso, G. Benedetto, P.A.G. Albo, D. Truong, D. Flack, in preparation
13. L. Pitre, private communication. The CMM data should be regarded as preliminary, but are sufficiently accurate for the purposes of this paper
14. J.D. Jackson, *Classical Electrodynamics, 3rd edn* (Wiley, New York, 1999)